# Analysis of slip transmission at grain boundaries in Alloy 600

Daeyeop Kwon, Jae Phil Park, Chi Bum Bahn*
*School of Mechanical Engineering, Pusan National Univ., Busan, 43241, South Korea*
**Corresponding author: bahn@pusan.ac.kr*

## 1. Introduction

Stress corrosion cracking (SCC) has been reported several times in pressurized water reactor primary environments [1]. Therefore, the study of SCC initiation has become increasingly important. The metal microstructure is one of the critical factors influencing SCC initiation. Previous research has shown that slip discontinuity at grain boundaries (GBs) also affects SCC [2]. Since slip transmission can be predicted using the Luster-Morris parameter [3], it is worthwhile to try to find out any relationship between the Luster-Morris parameter and SCC initiation at GBs. Long-term goal of this study is to conduct SCC initiation testing in simulated PWR primary water environments, analyze cracked GBs, and determine the relationship between the GB microstructure and SCC initiation. However, as the first step, it was intended to investigate whether the Luster-Morris parameter has any relationship with slip discontinuity at GBs in polycrystal Ni alloy.

## 2. Methods and Results

### *2.1 Sample preparation*

The material examined was a 1-mm thick Alloy 600 (annealed to promote grain growth) plate, of which the chemical composition is listed in Table 1. The dimension of the test specimen is shown in Fig. 1. Dimensions of the specimen's gauge section are 4 mm wide, 1 mm thick and 12 mm long. The specimen (front and rear face) was mechanically polished with SiC papers up to 800 grit, followed by successive polishing with 3 μm diamond paste and colloidal silica for Electron Back Scatter Diffraction (EBSD) analysis. Figure 2 shows a proving-ring type test set-up with an assembled tensile specimen. The load is applied to the specimen by turning upper and lower nuts. The proving-ring type loading system was introduced for the SCC initiation testing in simulated PWR primary water environments.

Table I: Chemical composition of test material (wt.%)

| Ni | Cr | Fe | Mn |
|---|---|---|---|
| Bal. | 16.3 | 8.4 | 0.18 |
| Cu | Si | C | S |
| 0.037 | 0.37 | 0.072 | 0.004 |

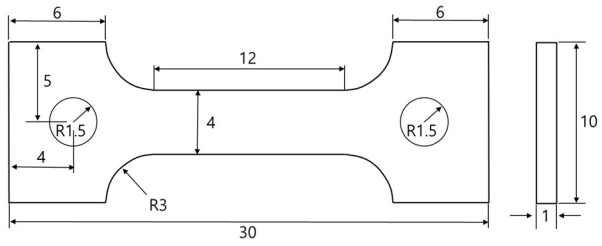


Fig. 1. Dimension of tensile specimen (mm)

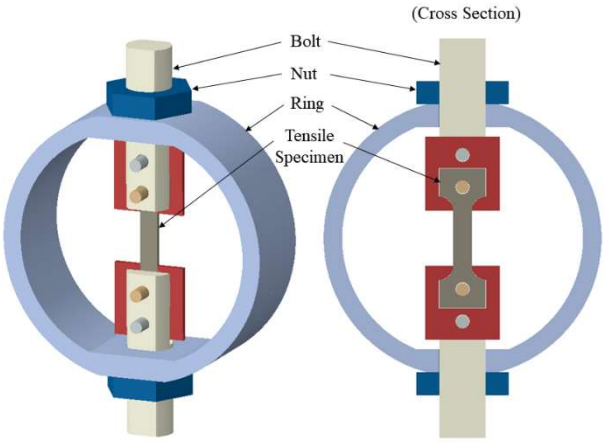


Fig. 2. Proving ring set-up

### *2.2 EBSD analysis*

EBSD analyses were performed on gauge sections of five specimens (#3, #4, #5, #6, and #7). Figure 3 shows an example of the inverse pole figure (IPF) maps of the #5 specimen prior to deformation. The IPF map shows that the grain size has increased by annealing from the initial size of 10-20 μm to 1-2 mm. EBSD analyses can also provide information about the crystal orientations, which can be used to determine misorientation angles at GBs and slip transmission parameters. The software MTEX [4] was used to analyze EBSD data and calculate microstructure characterization.

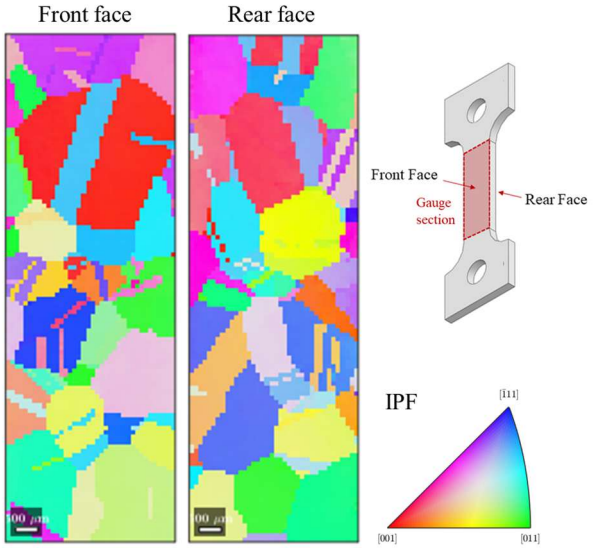


Fig. 3. Example of IPF maps of #5 specimen gauge sections prior to deformation

*2.3 Slip transmission parameter*

Slip continuity at GB can be predicted using the Luster-Morris slip transmission parameter [5]. The geometric parameters to predict the slip transmission between the two slip systems on both sides of the GB are defined as in Fig. 4. κ is the angle between slip directions, and ψ is the angle between slip plane normal directions. The Luster-Morris parameter was expressed by

$$m' = cos\psi \, cos\kappa \, . \quad (1)$$

When $m'$ equals to 1, GB is transparent from the slip transmission point of view. If $m'$ equals to 0, GB is an impenetrable boundary. Slip continuity becomes highly likely as $m'$ closes to 1.

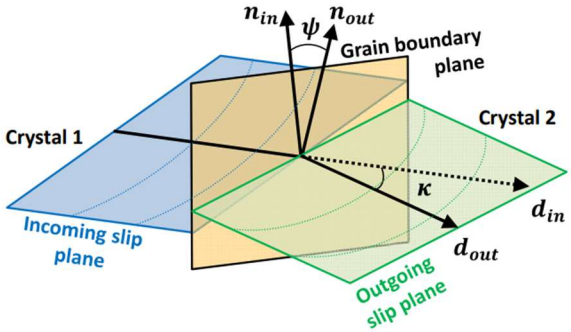


Fig. 4. Geometrical description of slip transmission [5].

*2.4 Slip transmission analysis*

Slip transmission was analyzed for 214 regular GBs in three specimens (#5, #6, #7). Figure 5 shows an example (optical microscope image) of slip continuity and discontinuity at GBs.

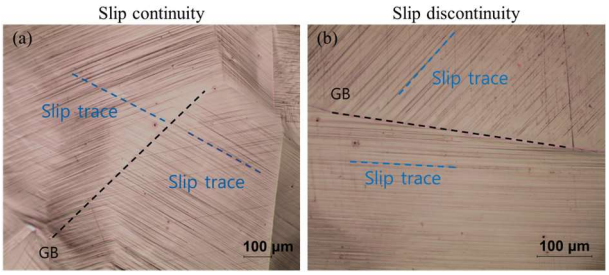


Fig. 5. Examples of slip continuity and discontinuity at regular GBs in #5 specimen.

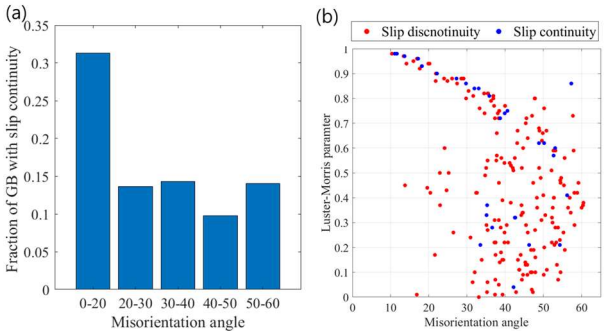


Fig. 6. (a) Effect of the misorientation angle on slip continuity for regular GBs. (b) GBs present slip continuity (blue dots) and slip discontinuity (red dots) as a function of the Luster-Morris parameter $m'$ and the misorientation angle.

As shown in Fig. 6a, slip continuity is mainly observed at GBs with low misorientation angle (0-20°). Figure 6b shows results of slip continuity/discontinuity at GBs as a function of the Luster-Morris parameter $m'$ and the misorientation angle. The probability of slip continuity at GBs is high when $m'$ is relatively large (larger than 0.8). However, the analysis results indicate that slip continuity was also observed at GBs with low $m'$ and high misorientation angle, which is somewhat different than expected. The reason for the difference between the predicted and experimental results appears to be the change in the crystal orientation after deformation induced by tensile loading. This change can lead to a prediction error of the slip system. The prediction is based on the EBSD results obtained before deformation.

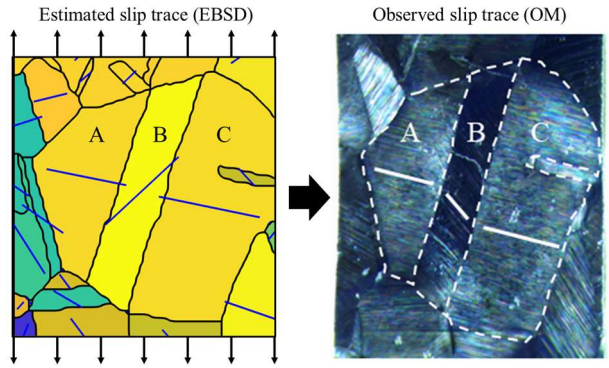


Fig. 7. Comparative example of estimated slip trace (blue line in left figure) from EBSD data set before deformation and observed slip trace (white line in right figure) after deformation in #5 specimen.

Figure 7 shows an example of the comparison between the estimated slip traces from the EBSD data obtained before deformation and observed slip traces after deformation at the same location. The estimated slip traces correspond to the observed slip traces for grains A and C, but not for grain B. Therefore, it is necessary to conduct the EBSD analysis on the test specimen after the deformation.

## 3. Conclusions and Future work

Earlier studies indicated that slip discontinuity affects SCC and that the Luster-Morris parameter can predict slip transmission. Therefore, this study intended to find out any relationship between the Luster-Morris parameter and slip continuity at GBs with polycrystal Ni alloy specimen. When the grain boundary orientation angle was relatively low, the probability of the slip transmission was relatively high and the Luster-Morris parameter was close to 1. However, the slip transmission also occurred when the orientation angle was high and the Luster-Morris parameter was low. To determine the relationship, if any, between the Luster-Morris parameter and the slip transmission, the analysis needs to be conducted with EBSD data from deformed specimens, because the grain crystal orientation can be affected by deformation.

The SCC testing with proving-ring type systems has been conducted in simulated PWR primary water environments for about 1000 hours, but no crack was observed. The SCC testing will be continued, and the relationship between the Luster-Morris parameter and SCC initiation at GBs will be explored further.

## ACKNOWLEDGEMENTS

This work was supported by the National Research Foundation of Korea (NRF) grant funded by the Ministry of Education (NO. 2018R1D1A3B0705066514), the Korea Institute of Energy Technology Evaluation and Planning (KETEP) and the Ministry of Trade, Industry & Energy (MOTIE) of the Republic of Korea (No. 20214000000410).

## REFERENCES

[1] P. Scott, M.-C. Meunier, Materials Reliability Program: Review of Stress Corrosion Cracking of Alloys 182 and 82 in PWR Primary Water Service (MRP-220), EPRI, Palo Alto, CA, 2007. Report No. 1015427.

[2] West, E. A., and G. S. Was. "Strain incompatibilities and their role in intergranular cracking of irradiated 316L stainless steel." *Journal of nuclear materials* 441.1-3 (2013): 623-632.

[3] Luster, Jörg, and M. A. Morris. "Compatibility of deformation in two-phase Ti-Al alloys: Dependence on microstructure and orientation relationships." *Metallurgical and Materials Transactions A* 26.7 (1995): 1745-1756.

[4] BACHMANN, F.; HIELSCHER, Ralf; SCHAEBEN, Helmut. Texture analysis with MTEX–free and open source software toolbox. In: *Solid state phenomena*. Trans Tech Publications Ltd, 2010. p. 63-68.

[5] Mercier D, Zambaldi C, Bieler T R 2014 STABiX, http://github.com/czambaldi/stabix